

Coupling of near-bottom pelagic and benthic processes at abyssal depths in the eastern North Pacific Ocean

K. L. Smith, Jr., R. S. Kaufmann, and R. J. Baldwin

Marine Biology Research Division, 0202, Scripps Institution of Oceanography, UCSD, La Jolla, California 92093

Abstract

A time-series site was established in the eastern North Pacific Ocean to study the coupling between near-bottom pelagic and benthic processes at abyssal depths in an area with well-documented seasonality in surface water productivity. Particulate total mass (PTM), particulate organic C (POC), particulate total N (PTN), and particulate calcium carbonate [$P(\text{CaCO}_3)$] fluxes were measured from sediment trap collections at 600 and 50 m above bottom from February 1990 to October 1991 (606 d). The sea floor at 4,100 m was concurrently monitored with a time-lapse camera over a 386-d period from July 1990 to July 1991. During this study, *in situ* measurements of sediment community oxygen consumption (SCOC) were made and surface sediment samples collected seasonally with a free-vehicle grab respirometer. PTM, POC, PTN, and $P(\text{CaCO}_3)$ fluxes exhibited a strong seasonal signal, with episodic peaks from spring through fall and lows in winter. SCOC increased sharply between winter and summer, coinciding with spring peaks in particulate fluxes. Detrital aggregates appeared on the sea floor in pulses over a 6-month period from July to December 1990, coinciding with periods when particulate fluxes were elevated but delayed ~1.5 months after the initial peaks in particulate flux. Mobile epibenthic megafauna monitored with time-lapse photography consisted primarily of holothuroids and echinoids and were twice as active when detrital aggregates were observed on the sea floor as during the rest of the year. Our results show a temporal relationship between the flux of particulate matter entering the benthic boundary layer, the arrival and residence of detritus on the sea floor, and the activity of the sediment community and mobile epibenthic megafauna.

The importance of long time-series studies for examining temporal variation in marine communities is widely accepted (e.g. Cushing 1982; Heip et al. 1987; Likens 1989). However, when studying remote and relatively inaccessible deep-sea communities, one must often rely on "snapshot" sampling and short time-series measurements to piece together a meaningful scenario of how these systems function on time scales exceeding that of a single cruise (≤ 1 month). Although seasonal

observations have shed much light on the temporal variability of biological processes in the deep sea (see Tyler 1988; Gage 1991), it has been difficult to understand many aspects of the functioning of these communities without a "continuous" record of certain biologically significant processes. Independent long time-series measurements of the flux of particulate organic matter to abyssal depths (e.g. Deuser et al. 1981; Deuser 1986; Honjo 1982) and time-lapse photographic records of phytodetritus reaching the sea floor (e.g. Billett et al. 1983; Lampitt 1985; Rice et al. 1986), although taken in widely separated geographic areas of the deep ocean, have been invaluable for interpreting short time-series measurements.

Some of the questions we have been trying to answer deal with the coupling between a pelagically derived food supply and its utilization by benthic communities in the deep sea (e.g. Smith 1987, 1992; Smith et al. 1992). Such pelagic-benthic coupling has been shown to coincide with organic detritus reaching the sea floor, as described in shallower coastal (e.g. Townsend and Cammen 1988), bathyal (Graf 1989), and abyssal (Pfannkuche and Lochte 1993) environments.

Acknowledgments

We thank J. Edelman, A. Genin, B. McCluskey, M. Olsson, W. Stockton, and W. Wakefield for assistance in developing the time-lapse camera instrument and the digitizing system. J. Edelman, B. McCluskey, T. Shaw, and R. Wilson were invaluable in handling the free-vehicle systems at sea. C. Reimers (supported by NSF grant OCE 89-11268) ran the carbon analysis of the sediment trap material from the earlier cruises in the time series and answered many of our analytical questions concerning sediment analyses. D. Pawson identified the echinoderms and J. Bauer, S. Beaulieu, A. Carlucci, A. Leonard, L. Lewis, I. Priede, C. Reimers, T. Shaw, P. Williams, and two anonymous reviewers provided discussions and comments on the manuscript.

We acknowledge support from NSF grant OCE 89-22620 to conduct the research and the Vetelsen Fund for support to develop the time-lapse camera systems.

The lack of long time-series measurements for the concurrent examination of the input of particulate matter to the deep-sea benthic boundary layer and its impact on the sea floor prompted us to establish a permanent abyssal study site in the eastern North Pacific. Over the past 3 yr, we have been studying the benthic boundary layer community at this site with long time-series monitoring of particulate matter flux and time-lapse photography combined with seasonal measurements of sediment community oxygen consumption and sediment chemistry. Here, our analysis has been confined to a 606-d period—part of the longer ongoing time-series study of benthic boundary layer processes at this station—to address two questions. Is there a temporal relationship (coupling) between the flux of particulate matter entering the benthic boundary layer and the arrival and residence of detritus on the sea floor? Is there a temporal relationship between the arrival and residence of detritus on the sea floor and the response of the benthic community (sediment community and epibenthic megafauna)?

Materials and methods

Area of investigation—This study was conducted at a single abyssal site (Sta. M: 34°50'N, 123°00'W; 4,100-m depth) in the eastern North Pacific, 220 km west of the central California coast (synonymous with Sta. N of Reimers et al. 1992). Surface waters of the California Current overlying this site have well-developed spring chlorophyll plumes that persist into summer (e.g. Smith et al. 1988; Michaelsen et al. 1988) and exhibit interannual variability in phytoplankton pigments (Pelaez and McGowan 1986).

Our study was confined to the bottom 600 m of the water column and the sediments, an area we refer to as the benthic boundary layer. Current velocity measured over 3–10-d intervals at 2, 50, and 600 m above bottom (mab) with moored current meters (SIO, model 6) during seasonal cruises (February, June, and October 1990 and February, June, July, August, and October 1991) exhibited a strong semidiurnal component with no obvious seasonal trends in either speed or direction. Speeds were highest at 50 mab ($\bar{x} = 3.8 \pm 2.8 \text{ cm s}^{-1}$; range, 0–18.2 cm s^{-1}), with decreased flow rates at 600 mab ($\bar{x} = 2.3 \pm 1.5 \text{ cm s}^{-1}$; range, 0–9.0

cm s^{-1}) and 2 mab ($\bar{x} = 2.7 \pm 1.6 \text{ cm s}^{-1}$; range, 0–8.2 cm s^{-1}). Casts with a transmissometer showed a noticeable decrease in light transmission beginning between 100 and 200 mab and extending to the bottom (Fig. 1A). There were no evident changes in light transmission detectable between February and July; no transmissometer casts were made in October 1990 or 1991. A 3-month deployment of the transmissometer between July and October 1991 at 1 mab revealed increased particle interference in August (Fig. 1B). Measurements of bottom-water dissolved oxygen concentrations at this station ranged from 142 to 146 $\mu\text{mol liter}^{-1}$ (Smith et al. 1992), and the sediment pore waters had detectable oxygen to ~3-cm depth (Reimers et al. 1992). In this area, the sea floor has low relief (<60 m over 770 km^2) and is composed of silty-clay sediments.

Particulate fluxes—Fluxes of particulate total mass (PTM), particulate organic C (POC), particulate total N (PTN), and particulate calcium carbonate [$\text{P}(\text{CaCO}_3)$] were measured from sediment trap collections between 26 February 1990 and 24 October 1991 (606 d). Sediment traps were moored at 600 and 50 mab, above and within the bottom layer of increased turbidity, respectively (Fig. 1). The initial 30-d sampling resolution was increased to 10 d beginning in June 1990 at 600 mab and in October 1990 at 50 mab (363 d with equal sampling resolution at both depths). These traps were recovered every 4 months, serviced, and then redeployed.

Each sediment trap consisted of a steep-sided funnel (Teflon-coated fiberglass cone; 120 cm long, 57-cm diam) with an effective mouth opening of 0.25 m^2 (Bruland et al. 1981) and was configured as a single trap with swiveled bridle. A baffle constructed of 1- × 1- × 5-cm-deep cellular grid (Hexcel) was set in the top of each funnel to reduce turbulence. An assembly of sequencing collection cups bolted to the bottom of each funnel was capable of flushing on descent and ascent and taking 12 discrete samples at depth (Honjo and Doherty 1988). Prior to June 1990 at 600 mab and October 1990 at 50 mab, sequencers with four sampling cups were used (developed at Oregon State University; see Smith 1987). Collection cups were filled before each deployment with water obtained from the deployment depth and

passed through precombusted GF/C filters. Each collection cup was poisoned with a filtered HgCl_2 solution (3.0 mM final concn).

On recovery of the sediment traps, "swimmers" were removed from each collection cup, visible observations of the material were recorded, and the remaining sample was resuspended and split into four equal-volume subsamples using an OSU splitter with a sampling precision of $\pm 7\%$ by mass (Dymond et al. 1981; Fischer 1984). Subsamples were immediately frozen at -20°C at sea, then transferred to a -70°C freezer for storage in the laboratory after each cruise.

In the laboratory, one frozen subsample from each 30-d collection cup and three combined subsamples from each 10-d collection cup were thawed and centrifuged. The supernatant was decanted and the remainder lyophilized, weighed, and ground to a fine powder with an agate mortar and pestle. Total dry mass was calculated after we estimated the salt content of weighted samples from their chloride content (determined by AgNO_3 titration, Strickland and Parsons 1972). Each subsample was analyzed in duplicate for total C and N (Perkin-Elmer 2400C elemental analyzer) and for inorganic C (Coulometrics carbon analyzer) with corrections for salt content. CaCO_3 was calculated by multiplying the inorganic C fraction by the formula weight of CaCO_3 divided by the molecular weight of C. Organic C was calculated as the difference between the total and inorganic C fractions. N concentration was not corrected for the inorganic fraction (sorbed and fixed ammonia), yielding total N (inorganic + organic fractions).

Sinking fluxes of PTM, POC, PTN, and $\text{P}(\text{CaCO}_3)$ were calculated ($\text{m}^{-2} \text{d}^{-1}$). Corrections for POC and PTN dissolution over the incubation period (as determined by comparison of DOC and DON in initial and final water samples from collection cups) are not presented here because of their minor impact on POC (Smith et al. 1992) and PTN (P. M. Williams unpubl. data) at this station.

In analyzing the particulate fluxes, a Wilcoxon paired-sample test (Zar 1984) was used to examine the differences between rates at 50 and 600 mab for periods up to 606 d. For this test, we used only those measurements for which paired samples were collected over the same sampling intervals. Estimates of partic-

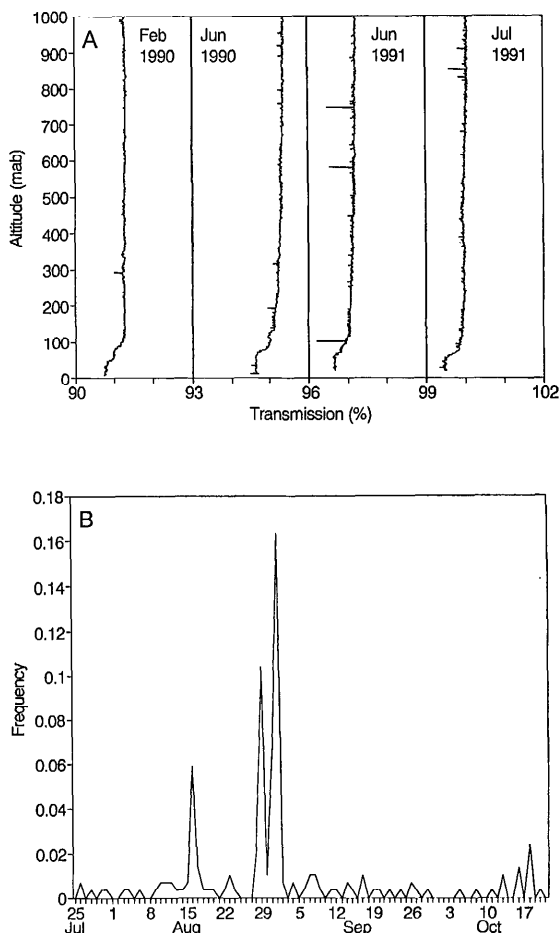


Fig. 1. A. Transmissometer depth profiles in the bottom 1,000 m of the water column at Sta. M for casts made in February and June 1990 and June and July 1991. Air calibration data for February and June 1990 are not available so transmission percentages are relative values and not directly comparable to later casts. B. Time-series profile of light transmission over a 3-month period from 25 July to 21 October 1991 at 1 mab at Sta. M. A Sea Tech transmissometer (25-cm path; Bartz et al. 1978) with SeaBird data logger, used for the seasonal profiling casts, was air calibrated and mounted horizontally 1 mab on a free-vehicle camera tripod for the 3-month deployment. Individual light transmission readings (taken once every 5 min = 288 times d^{-1}) were compared to a 12-h running mean of light transmission readings (baseline consisting of transmission readings for 6 h before and after a given time point). Individual readings differing from the baseline by $>0.50\%$ (light transmission was measured on a continuous scale from 0 to 100%) were tabulated on a daily basis and divided by the total number of readings taken each day (288; see above), yielding a frequency.

ulate fluxes were derived from integrations of the flux curves for periods of 60–606 d, using an electronic digitizer (Science Accessories Corp.) interfaced with a personal computer equipped with Sigma Scan (Jandel Scientific Corp.). The digitizing error (SD) in 5 replicates of each integrated period was $\pm 5\%$.

Sea-floor monitoring—Time-lapse photographs of the sea floor were taken at hourly intervals from July 1990 through July 1991 (386 d) with a free-vehicle camera tripod system described by Smith et al. (1993). This camera system consisted of a tripod frame with a time-lapse camera (Benthos model 377) mounted obliquely in its apex and two 400 W-s strobes, one mounted on each side of the camera. Oblique mounting of the camera and strobes provided a well-illuminated field of view covering $\sim 20 \text{ m}^2$. The camera was loaded with color negative film (Fuji, type 8514, 500 ASA) and programmed to take hourly photographs of the sea floor over a 4-month period. Due to a technical problem, photographs were taken at 4-h intervals during the 4-month period from October 1990 to February 1991.

Oblique photographs taken with the free-vehicle camera system were analyzed with a perspective grid method (Wolf 1983; Wakefield and Genin 1987). Each photograph was projected onto a flat surface. The objects in each photograph were tentatively identified and then digitized with an electronic digitizer (*see above*) interfaced with a computer. A computer program was developed to measure the sizes and positions of objects on the sea floor with this system (Wakefield and Genin 1987). A scale marker was lowered into the field of view (Smith et al. 1993) between October 1990 and February 1991 to calibrate the geometry of the camera (elevation and inclination). This system yielded photographs with a maximum sea-floor resolution of 3 mm on the *X*-axis and 5 mm on the *Y*-axis.

Digitized data were analyzed by treating sequential photographs as serial observations of a semicircular area with the camera at its center (Buckland et al. 1993). The radial distance of each object from the bottom center of each photograph was computed, and a probability density function was fitted to the observed distribution of distances with the computer program DISTANCE (Laake et al. 1991). The

probability density function describes the spatial distribution of objects as a function of distance from the camera and can be used to estimate object densities. From the output generated by DISTANCE, we determined densities of animals and features.

The area of sea floor over which detrital aggregates and megafauna were visible depended primarily on the size and color of the objects with respect to the sediment (Kaufmann et al. 1989). In general, objects that were translucent or whose color closely resembled that of the surrounding sediment were difficult to discern in areas of suboptimal lighting (close foreground and distant background), while objects whose color or texture contrasted markedly with that of the sediment were identifiable over a much larger area. The probability density function was used to calculate the effective observation area for each species, a parameter dependent on the relative visibilities of objects in photographs (*see* Smith et al. 1993). The densities of all objects were normalized to a 20-m^2 area (the approximate field of view of the camera) for comparative purposes.

The total percentage of sea floor covered by detrital aggregates during a given time period was calculated with a computer program to plot the position and areal coverage of each detrital aggregate observed on the sea floor. Positions of aggregates in successive photographs were compared to previously plotted positions and considered different if their centers were outside the area covered by a previously observed aggregate. This procedure was repeated until all aggregates observed during a photographic series had been treated. The total area covered by the aggregates was then divided by the effective area viewed (20 m^2) to yield percent coverage for a given period of time (1 h–1 yr).

Sediment sampling—Seasonal measurements of sediment community oxygen consumption (SCOC), as an estimate of the mineralization rate of organic C, were made in situ over 2-d intervals with a free-vehicle grab respirometer (Smith 1987). The free-vehicle grab respirometer was deployed twice on each cruise from February 1990 through June 1991, then once per cruise from July through October 1991. This instrument consisted of flotation mounted above an aluminum frame that sup-

ported a central instrument package and a tray with four stainless-steel grabs; the grabs were slowly pushed ~15 cm into the sediment after the free vehicle reached the sediment surface. Each grab was equipped with a stirring motor to continuously circulate the water above the sediment, simulating natural boundary conditions and creating a flow of water over a polarographic oxygen sensor. The output from the oxygen sensor in each grab was sampled every 15 min and the signal digitally recorded with a magnetic tape drive housed in a pressure cylinder. Each sensor was calibrated with chilled, nitrogen-purged and oxygen-saturated seawater as limits, and the SCOC was calculated for each grab by the methods described by Smith (1987). SCOC was converted to organic C utilization, assuming a respiratory quotient of 0.85 (mixed carbohydrate and lipid; Brody 1945) and yielding rates in $\text{mg C m}^{-2} \text{d}^{-1}$.

A sediment core was taken from one grab of the free-vehicle grab respirometer during each cruise and sectioned in a cold room at 2.5-mm intervals in the upper 10 mm. Conspicuous organisms were removed from each section. Subsamples from each sediment section were extracted in 0.5 M H_3PO_4 and analyzed in triplicate for ATP (Craven et al. 1986). Internal ATP standards were added to an additional subcore at each depth to estimate adsorptive and other losses of extracted ATP (Karl and Craven 1980; Craven and Karl 1984). Chlorophyll *a* and pheopigments were also analyzed in triplicate from each sediment section by the method of Parsons et al. (1984). Dry weight of the sediment at each depth interval was determined on another set of triplicate subcores and corrected for salt concentration by AgNO_3 titration (Strickland and Parsons 1972). Additional sediment from each section was frozen at -20°C , then transferred to a -70°C freezer for later duplicate analysis of total N, total C (Reimers et al. 1992), and inorganic C (Reimers and Smith 1986).

Collections of epibenthic megafauna were made with a semiballoon trawl (5-m foot rope; 3.8-cm stretch mesh with 1.3-cm-mesh cod-end liner) at the beginning and end of each time-lapse camera deployment. Specimens were preserved in 10% buffered Formalin and identified by appropriate specialists to provide

tentative identifications for animals observed in the time-lapse photographs.

Results

Particulate fluxes—PTM, POC, PTN, and $\text{P}(\text{CaCO}_3)$ fluxes exhibited strong seasonal patterns at both 600 and 50 mab, with peaks from spring through fall and lows in winter over a period from February 1990 to October 1991 (606 d) (Fig. 2). However, there was a striking degree of variation between years, with a substantial increase in the PTM, POC, PTN, and $\text{P}(\text{CaCO}_3)$ fluxes in spring and summer 1991 compared to the previous year. In 1990, there was a sustained period of elevated PTM, POC, PTN, and $\text{P}(\text{CaCO}_3)$ fluxes beginning in March and lasting through summer. By comparison, during 1991, the spring pulse in these fluxes did not begin until April and had two major peaks—April and May—before declining to a minor resurgence in July, followed by a decrease in August.

To examine the quality of the particulate fluxes, we calculated POC:PTM, POC:PTN, and $\text{P}(\text{CaCO}_3)$:PTM. The ratio of POC flux to PTM flux ranged from 0.04 to 0.19 and was higher and more variable in fall and winter (Fig. 3). POC flux:PTN flux was also highly variable from fall through early spring and ranged from 7.2 to 15.6, with no discernible temporal patterns at either 600 or 50 mab. $\text{P}(\text{CaCO}_3)$ flux:PTM flux ranged from 0.17 to 0.53 over the 606-d period and was most variable in winter and early spring (Fig. 3).

Peaks in PTM, POC, PTN, and $\text{P}(\text{CaCO}_3)$ fluxes were generally coincident between 600 and 50 mab but endured for a longer period at 50 mab. A Wilcoxon paired-sample test was used to test the difference between fluxes at 50 and 600 mab for the 606-d period. Particulate fluxes were significantly higher at 50 than at 600 mab for PTM [$T < T_{0.01(2),39} = 207$; $T = 128$], POC [$T < T_{0.01(2),39} = 207$; $T = 157$], PTN [$T < T_{0.01(2),39} = 207$; $T = 160$], and $\text{P}(\text{CaCO}_3)$ [$T < T_{0.01(2),38} = 194$; $T = 155$]. For this statistical test, we have assumed the temporal difference between the 600- and 50-mab fluxes to be negligible over the sampling interval (10 or 30 d). We used the same statistical test to compare the 363-d period (26 October 1990–24 October 1991) when the sampling resolution was the same (10 d) at both 600 and

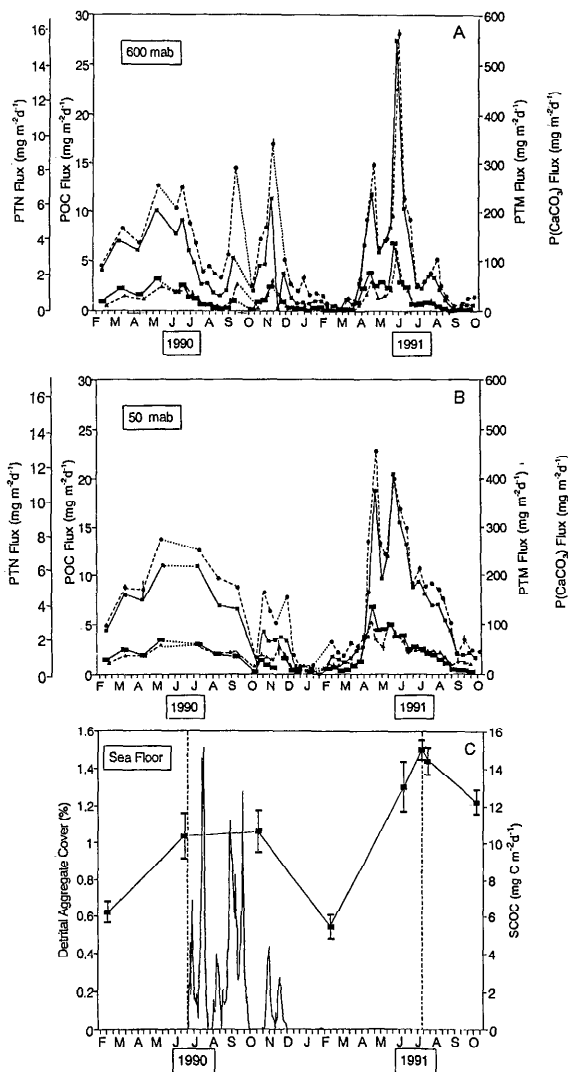


Fig. 2. A, B. Fluxes of particulate total mass (PTM: solid line ■), particulate organic C (POC: dashed line ●), particulate total N (PTN: dashed line ▲) and particulate CaCO₃ [P(CaCO₃): solid line ■] at 600 and 50 mab compared with detrital aggregate cover (%) observed on the sea floor from February 1990 to October 1991. The POC, PTN, and P(CaCO₃) fluxes at 600 and 50 mab, reported as part of a long time series by Smith et al. (1992), were determined in duplicate and are presented as maximum, minimum, and mean. PTM fluxes are based on single determinations for each sampling period. Dotted lines indicate periods when no sample was taken or the sample was of insufficient size for complete analysis. C. The percentage of the sea floor covered by detrital aggregates was determined for a photographic area of 20 m² from 1 July 1990 to 22 July 1991 (386 d; bounded by dashed lines). Time-lapse photographs of the sea floor were taken at hourly intervals with a free-vehicle camera tripod system which was serviced every 4 months. This servicing

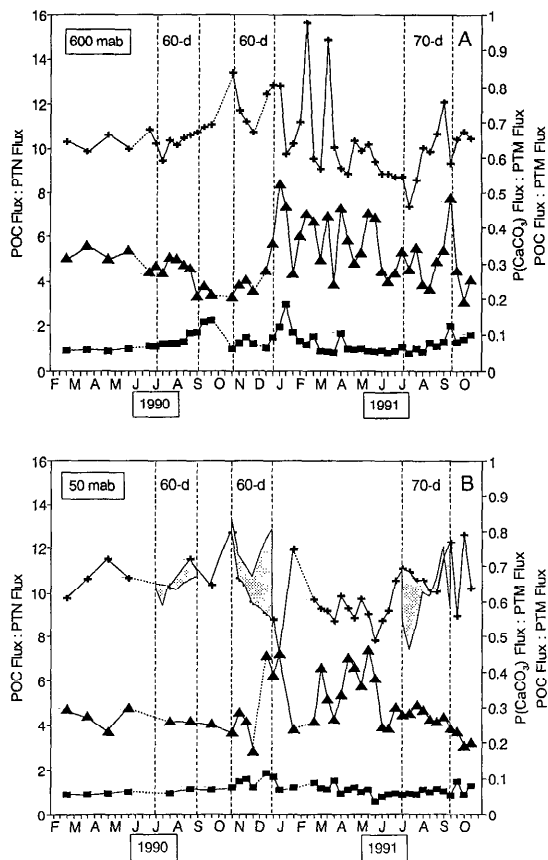


Fig. 3. Ratios of POC flux to PTM flux (■), POC to PTM flux (+), and P(CaCO₃) flux to PTM flux (▲) at 600 and 50 mab from June 1990 to October 1991. Dotted lines between points indicate periods when no measurements were available. Shaded areas on 50-mab plot represent differences between synoptically measured ratios from 600- and 50-mab traps during selected 60- and 70-d periods (see Table 1). Month designation on lower axis represents first day of each month.

50 mab. Again, the particulate fluxes were significantly higher at 50 mab than at 600 mab for PTM [$T < T_{0.01(2),32} = 128$; $T = 105$], POC [$T < T_{0.01(2),32} = 128$; $T = 99$], PTN [$T <$

←
created gaps in the data of 5 d between 24 and 28 October 1990, 16 d between 18 February and 5 March 1991, and 17 d between 7 and 23 June 1991. Sediment community oxygen consumption (SCOC) values are plotted with the detrital aggregate cover and represent mean rates with ± 1 SD (SCOC measurements were reported as part of a long time series by Smith et al. 1992). Month designation on lower axis represents first day of each month.

Table 1. Particulate fluxes [PTM, POC, PTN, P(CaCO₃)] and flux ratios [POC:PTM, POC:PTN, P(CaCO₃):PTM] estimated from integration of the particulate flux curves for four sampling periods.

Integrated sampling period	Altitude (mab)	Fluxes				Flux ratios		
		g m ⁻² (sampling period) ⁻¹				POC:PTM (wt)	POC:PTN (M)	P(CaCO ₃):PTM (wt)
		PTM	POC	PTN	P(CaCO ₃)			
606 d (26 Feb 1990–24 Oct 1991)	600	57.74	3.96	0.46	16.28	0.07	10.03	0.28
	50	80.20	4.99*	0.56	22.59	0.06	10.40	0.28
60 d (7 Jul–5 Sep 1990)	600	5.69	0.42	0.05	1.59	0.07	9.72	0.28
	50	12.58	0.76	0.08	3.23	0.06	10.50	0.26
60 d (26 Oct–25 Dec 1990)	600	7.00	0.54	0.05	1.68	0.08	12.50	0.24
	50	3.87	0.37	0.04	1.06	0.09	10.62	0.27
70 d (6 Jul–14 Sep 1991)	600	4.37	0.27	0.03	1.06	0.06	10.71	0.24
	50	10.07	0.62	0.06	2.63	0.06	12.02	0.26

* POC fluxes corrected from Smith et al. (1992) where values were 75% lower due to digitizer calibration error; estimate does not include the addition of the dissolved organic C fraction which is presented by Smith et al. (1992) for this period at 50 mab.

$T_{0.01(2),32} = 128$; $T = 100$], and P(CaCO₃) [$T < T_{0.01(2),32} = 128$; $T = 90$].

The quality of the particulate fluxes between 600 and 50 mab was also examined. Differences in POC flux:PTM flux between sampling depths were most pronounced in September 1990 and 1991, when the flux was greater at 600 than at 50 mab. However, there was no significant difference in this ratio between 600 and 50 mab over the 606-d period [$T > T_{0.05(2),38} = 235$; $T = 332$]. There was also no significant difference [$T > T_{0.05(2),39} = 249$; $T = 354$] in the POC:PTN between the fluxes measured at 600 and 50 mab over the 606-d period. However, there were obvious departures in the POC:PTN during summer and fall, coinciding with the period when the discrepancies in fluxes between 600 and 50 mab were greatest. There were higher ratios in fall (October–December 1990) and lower values in summer (July–September 1990 and 1991) at 600 than at 50 mab (Fig. 3). There was no significant difference in the P(CaCO₃) flux:PTM flux between 600 and 50 mab [$T > T_{0.05(2),38} = 235$; $T = 364$] and no obvious seasonal disparity between depths.

To further examine the difference between particulate fluxes at 600 and 50 mab, we integrated the flux curves (Fig. 2) over the 606-d sampling period as well as over several shorter intervals when the greatest disparity occurred between sampling depths. The PTM and P(CaCO₃) fluxes at 50 mab were both 39% greater than those fluxes at 600 mab over the 606-d sampling period (Table 1). Similarly, the POC and PTN fluxes were, respectively, 26 and 22% greater at 50 mab than at 600. The

greatest discrepancy between the fluxes at 600 and 50 mab occurred in summer 1990 and 1991 (Fig. 2). Integration of the flux curves for a 60-d period between 7 July and 5 September 1990 revealed that the PTM, POC, PTN, and P(CaCO₃) fluxes were greater by 121, 81, 60, and 103% at 50 mab than at 600 (Table 1). During a 70-d period between 6 July and 14 September 1991, the PTM, POC, PTN, and P(CaCO₃) fluxes were greater by 130, 130, 100, and 148%, respectively, at 50 mab. In contrast, there was one 60-d period in fall 1990 (26 October–25 December) when the fluxes were noticeably higher at 600 mab: PTM, POC, PTN, and P(CaCO₃) fluxes were elevated 81, 46, 25, and 58%, respectively, over those at 50 mab. The small sample sizes for these 60- and 70-d intervals did not permit an informative statistical comparison.

Detrital aggregates on the sea floor—Sea-floor monitoring with the time-lapse camera began on 1 July 1990 and ended on 22 July 1991 (386 d). Detrital aggregates (defined here as clumps of amorphous-looking particulate matter distinguishable in photographs by color, shading, or texture) first appeared on the sea floor in early July 1990, and there were five episodic pulses between July and early October (Fig. 2). This series of events was followed by a hiatus in October when no aggregates were present and then a reappearance of aggregates in two pulses beginning in early November. The detrital aggregates had disappeared from the sea floor by mid-December, and there were only sporadic sightings recorded until the end of the monitoring program in late July 1991.

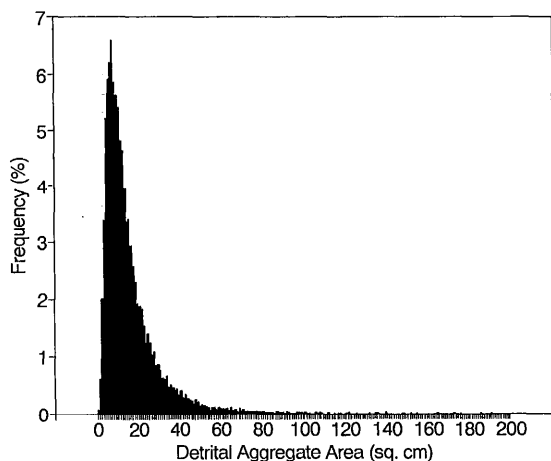


Fig. 4. Size-frequency distribution of detrital aggregates ($n = 15,616$ observations) digitized in time-lapse photographs of the sea-floor at Sta. M between July 1990 and July 1991.

Detrital aggregates appeared on the sea floor as amorphous-looking brown masses which were typically ellipsoid in shape and ranged in size from 0.6 to 191 cm² ($\bar{x} = 18$ cm²; 15,616 observations; Fig. 4). Digitized positions of individual detrital aggregates did not change appreciably (within the resolution limits of the digitizer) as they gradually blended in with and became indistinguishable from the surrounding sediment over <4 h–21.2 d ($\bar{x} = 45$ h). Although these detrital aggregates covered $<1.5\%$ of the sea floor seen in each photograph (~ 20 m²) at any one time (Fig. 2), collectively they covered 24.8% of the sea floor over the course of 1 yr.

Peaks in the coverage of detrital aggregates on the sea floor coincided with periods when particulate fluxes were elevated, particularly between July and early October (Fig. 2). However, the peaks in detrital aggregate coverage occurred ~ 1.5 months after the initial peaks in particulate fluxes in May, and no aggregates were observed on the sea floor during the previous 4-month period from February through June 1990 (K. Smith unpubl. data). Aggregations of particulate matter in the sediment trap collections were observed primarily in summer and fall when the POC flux : PTM flux was elevated (Fig. 3), coinciding with periods when detrital aggregates were observed on the sea floor. During summer, there were also much

higher fluxes of particulate matter at 50 mab than at 600. The absence of detrital aggregates on the sea floor in October 1990 corresponded to a decrease in particulate fluxes and was followed by secondary peaks in both aggregates and particulate fluxes in November and early December. Detrital aggregates did not reappear on the sea floor the following spring, despite the strong peaks in particulate fluxes during this period (Fig. 2). No detrital aggregates were observed throughout spring and early summer until the end of the monitoring program on 22 July 1991. Although there is circumstantial evidence to link the elevated particulate fluxes with the occurrence of detrital aggregates on the sea floor, a qualitative comparison was not possible because our cruises in 1990 did not overlap with the periods when aggregates were visible.

Sediment community oxygen consumption—We measured SCOC seasonally over the course of this sea-floor monitoring program as part of a longer time series of SCOC measurements reported by Smith et al. (1992). SCOC, as a measure of the mineralization rate of organic matter by the sediment community, increased significantly between February and June 1990 [Mann-Whitney U -test; $P < 0.05$; $U_{0.01(2),6,7} = 39$, $U = 42$], immediately preceding the first observations of detrital aggregates on the sea floor (Fig. 2). A similar pattern appeared the following year, when there was a sharp increase in SCOC between February and July 1991. The summer peak in SCOC in 1990 was lower than in 1991; June rates were 10.37 ± 1.21 mg C m⁻² d⁻¹ in 1990 and 13.06 ± 1.32 mg C m⁻² d⁻¹ in 1991. The June 1991 rate corresponded to elevated fluxes of particulate matter during spring and summer 1991 (Fig. 2). From these results, SCOC appears more closely aligned temporally with particulate fluxes than with the presence of detrital aggregates on the sea floor.

Sediment chemistry—Organic C was generally highest in the upper 2.5 mm of the sediment, ranging from 14.8 to 18.2 mg C (g dry wt)⁻¹ (Fig. 5A). The organic C concentration increased in fall and winter 1990 and showed a low the following June, temporally inconsistent with peaks in particulate fluxes (Fig. 2) but consistent with observed increases in POC : PTM during fall and winter 1990–1991 (Fig. 3). A similar temporal pattern occurred in total

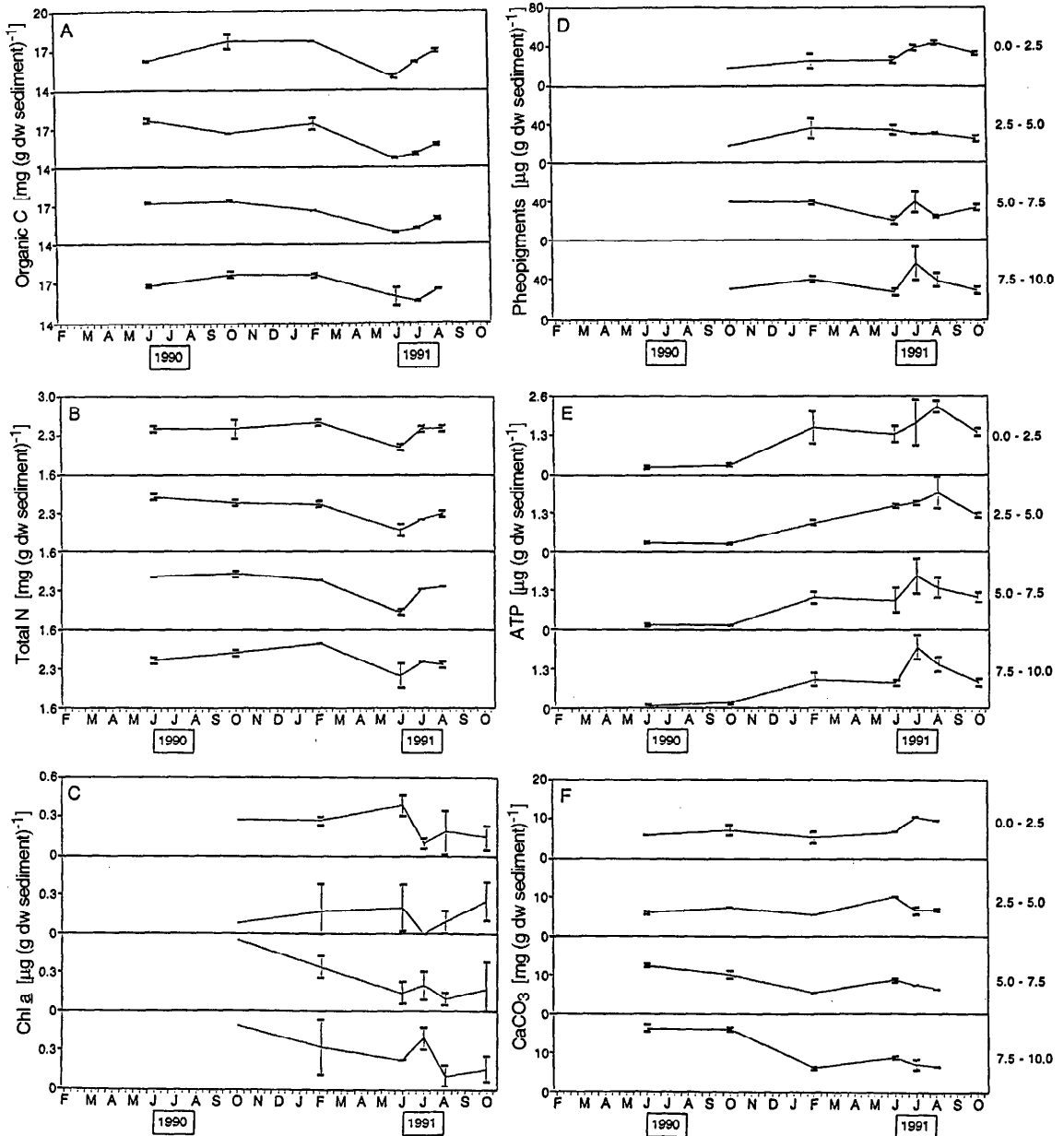


Fig. 5. Surface sediment profiles of organic C, total N, Chl *a*, pheopigments, ATP, and CaCO_3 at Sta. M between June 1990 and October 1991, measured over 2.5-mm depth intervals from the surface to 10-mm depth. (Depth interval indicated at right, month designation on lower axis represents first day of each month.)

N, which had a narrow range of 2.0–2.8 mg N (g dry wt)⁻¹ and exhibited a low in June 1991 (Fig. 5B).

In the upper 5 mm of the sediments, Chl *a* content increased between October and June before decreasing in July (Fig. 5C). Between 5-

and 10-mm depth, the peak in Chl *a* content shifted into July, suggesting a mixing phenomenon. Our sampling frequency was not sufficient to resolve any Chl *a* input to the surface sediments in the preceding 4-month period, between February and June 1991. Pheopig-

ment concentration in the upper 2.5 mm of the sediment increased gradually, from a low in October 1990 to a high in August 1991, but was more variable at greater depths, with earlier peaks in July (Fig. 5D).

ATP concentration in the surface sediments, as a measure of microbial biomass, increased from June 1990 to a maximum in August 1991 in the upper 5 mm and another maximum in July 1991 between 5- and 10-mm depth (Fig. 5E). These increases in ATP coincided with increased particulate fluxes and elevated SCOC in 1991 and specifically with the peak in SCOC during July and August 1991 (Fig. 2).

CaCO₃ ranged from 5.14 to 16.36 mg (g dry wt)⁻¹ in the upper 10 mm of the sediments (Fig. 5F). Concentrations of CaCO₃ were generally highest in summer, especially below 5 mm in 1990 and in the upper 2.5 mm in 1991.

Although there was considerable variation in the sediment parameters, it is interesting that Chl *a*, pheopigments, ATP, and CaCO₃ were generally highest in the surface sediments during summer 1991 (Fig. 5C–E), in concert with the highest fluxes in particulate matter and SCOC (Fig. 2), while organic C was highest in fall and winter (Fig. 5A), when particulate fluxes were low but the POC flux:PTM flux values were higher. The ratio of organic C to total N in the surface sediment exhibited little variation over the study period, ranging from 7.5 to 9.1, with the lowest values in June and July.

Mobile epibenthic megafauna—The mobile megafauna (defined as those animals which were visible in photographs taken with the time-lapse camera system and which displayed active horizontal movements across the sediment surface) were composed primarily of holothuroids and echinoids. Not included with the mobile megafauna are ophiuroids, which did not undergo discernible horizontal movements and were often buried in the sediment where their numbers and movements were obscured from photographic analysis (Smith et al. 1993).

Mobile megafauna at Sta. M collectively traversed up to 0.3 m² (body width × distance traveled) of the sea floor per day over a 20-m² area. We developed an index of activity based on the total area traversed by all mobile megafauna divided by the total number of mobile megafauna observed per day in the time-lapse

photographs and normalized to a sea-floor area of 20 m² with the formula

$$I = \sum_{j=1}^m \frac{\left(\sum_{i=1}^n D_i W_i \right)_j}{N_j A_j}$$

D_i is the distance travelled by organism i between two photographs, W_i the width of organism i , N_j the number of individuals of species j detected during the observation period, A_j the effective area viewed for species j , n the number of individuals of a given species exhibiting detectable movements across the sea floor during the observation period, and m the total number of mobile megafaunal species observed. I is expressed in units of area traversed per animal per unit area observed per unit time [in this case, cm² animal⁻¹ (20 m²)⁻¹ d⁻¹].

Mobile megafaunal activity by holothuroids (*Peniagone vitrea*, *Abyssocucumis abyssorum*, *Elpidia minutissima*, *Amperima* sp.) and echinoids (*Echinocrepis* sp.) was measured over the entire photographic monitoring period (July 1990–July 1991) and computed as a 10-d running mean over the 386-d interval. Megafaunal activity was generally twice as great during the time when detrital aggregates were visible on the sea floor as it was during the rest of the year (Fig. 6A,B). Activity declined sharply in November after the primary pulses of detrital aggregates and then increased episodically until June 1991, never reaching the peak values gained the previous fall. Increases in megafaunal activity generally followed peaks in detrital aggregate presence, suggesting that increased activity by these animals was induced by the presence of aggregates. We also found that individual mobile megafauna were occasionally associated with visible detrital aggregates. The high megafaunal activity in summer and fall 1990 was due primarily to an increased abundance of the numerically dominant holothuroid *A. abyssorum*, while in winter and spring, the holothuroid *P. vitrea* was most abundant (Fig. 6C).

Discussion

The temporal relationship between particulate fluxes through the bottom portion of the water column and the SCOC as a measure of carbon mineralization is strong in this data set

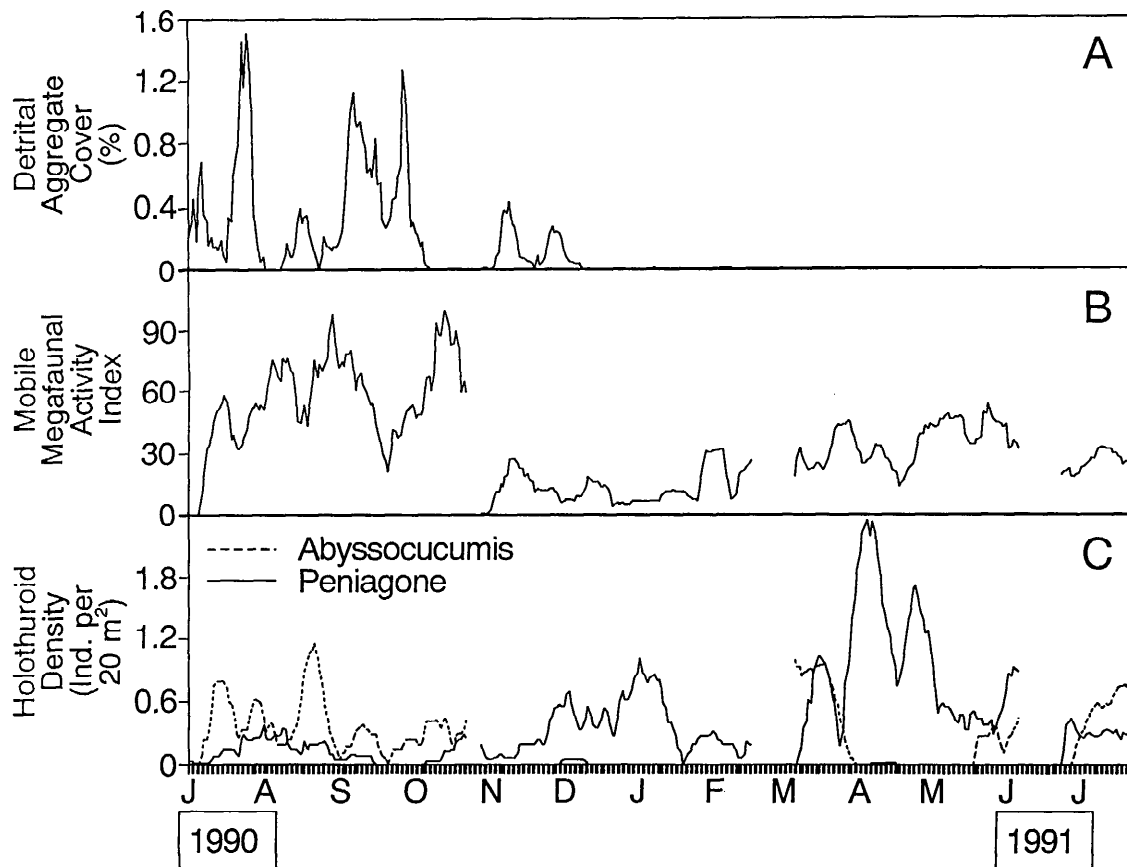


Fig. 6. Percent detrital aggregate cover on the sea floor compared with the mobile megafaunal activity index and the abundances of two dominant megafaunal species, the holothuroids *Abyssocucumis abyssorum* and *Peniagone vitrea*, over a period from 1 July 1990 to 22 July 1991. Time-lapse photographs from the camera tripod were analyzed for a 20-m² area of sea floor and 10-d running means computed over the 386-d monitoring period. Mobile megafaunal activity was calculated using the total area traversed by all mobile epibenthic animals (body width × distance traveled) divided by the total number of mobile megafauna observed per day and normalized to an area of 20 m² [units: cm² traversed animal⁻¹ (20 m²)⁻¹ d⁻¹]. This activity was primarily by holothuroids (*A. abyssorum*, *P. vitrea*, *Elpidia minutissima*, *Amperima* sp.) and echinoids (*Echinochrepis* sp.). Servicing of the camera tripod between deployments created gaps in the data (see Fig. 2 legend). Month designation on lower axis represents first day of each month.

(Fig. 2) and in the more extensive 2.3-yr data set from this same station (Smith et al. 1992). Microbial biomass (ATP) and Chl *a* in the surface sediments also exhibited peaks during summer that corresponded to those of SCOC, especially in 1991 when the most intensive sampling was done. We expected to measure similar fluxes of particulate matter at 600 and 50 mab, based on previous studies involving sediment trap collections in proximity to the sea floor (e.g. Honjo et al. 1992; Honjo and Manganini 1993). However, the quantitative difference between the sinking particulate mat-

ter at 600 and 50 mab and the apparent time lag between the initial pulses in particulate fluxes and the first appearance of detrital aggregates on the sea floor merit further consideration.

Water column—In summer, fluxes of particulate matter were greater at 50 than at 600 mab (Fig. 2), with lower POC : PTM (1990 and 1991) and higher POC : PTN (1991) at 50 mab (Fig. 3). There was also a decrease in light transmission within the bottom 200 m of the water column at Sta. M during all seasons measured (Fig. 1A), suggesting a persistent layer of

small suspended particles not measured with the sinking particulate flux collected in the sediment traps (Asper et al. 1992; Walsh and Gardner 1992). During the 4-month deployment of the transmissometer at 1 mab from July to October 1991, there were more frequent interruptions in light transmission during August than at any other time (Fig. 1B), indicating larger particles than those constituting the background of suspended particles. Such observations can be explained by processes such as lateral advection, bottom resuspension, or oversampling of particulate matter by sediment traps at 50 mab. Each of these possibilities is discussed below.

Lateral advection of particulate material is likely at this station because of the proximity of the station to the continent (e.g. Honjo et al. 1982; Walsh and Gardner 1992). Transport of particulate matter to the continental rise from the shelf and slope in nepheloid layers, debris flows, and turbidity currents has been suggested to explain benthic carbon demands exceeding either measured or estimated supplies from sinking particulate matter at a series of stations between 3,300- and 3,750-m depth to the immediate north and east of our station (Reimers et al. 1992).

Integrated particulate fluxes over the 606-d period reported here also show a pronounced increase in PTM (39%) and $P(\text{CaCO}_3)$ (39%) as well as in POC (26%) and PTN (22%) at 50 mab compared to 600 mab (Table 1). These discrepancies were most pronounced between July and September in both 1990 and 1991 but occasionally reversed, as in fall 1990 (Table 1, 26 October–25 December), when fluxes were higher at 600 than at 50 mab. Smith et al. (1992) integrated the POC fluxes at 600 and 50 mab over an 852-d period from June 1989 through October 1991 at Sta. M, 246 d of which were immediately before the 606-d period reported here. They found that the POC fluxes at these two depths agreed to within 4%, suggesting that lateral advection is not important at Sta. M. However, the 246-d period consisted of only four flux measurements at 600 mab and six flux measurements at 50 mab, and this limited sampling may have biased the results.

Similar increases in total particulate and organic C fluxes in proximity to the sea floor have been reported seasonally for organic C in the Panama Basin (Honjo 1982) and annually

for total particulate and organic C (Walsh et al. 1988) in the north equatorial Pacific. These increases in the north equatorial Pacific have been attributed to resuspension of rebound particles, defined as those particles that have not become incorporated into the sediments (Walsh et al. 1988) or changed in bulk chemical properties (Walsh and Gardner 1992). These macroaggregates are generally between 0.5 and 10 mm in diameter (Asper 1987; Gardner and Walsh 1990) and, as rebound particles, can be resuspended at lower current speeds from those required for fine-grained bottom sediments (Walsh et al. 1988). At Sta. M, the maximum current speed recorded at 2 mab was 8.2 cm s^{-1} ($\bar{x} = 2.7 \text{ cm s}^{-1}$), barely exceeding the minimum current speed necessary to resuspend phytodetritus in the abyssal eastern North Atlantic (7 cm s^{-1} , Lampitt 1985). By comparison, current speeds $>12 \text{ cm s}^{-1}$ are necessary to resuspend clay sediments in the Pacific (Lonsdale and Southard 1974; Gardner et al. 1984). We have observed higher POC:PTM and lower POC:PTN in fluxes at 600 than at 50 mab during a few isolated periods in summer lasting $<30 \text{ d}$ (Fig. 3), suggesting resuspension events with an input of more refractory organic matter at 50 mab. However, when particulate fluxes are integrated over summer periods of 60 d in 1990 and 70 d in 1991, the resulting ratios [POC:PTM, POC:PTN, $P(\text{CaCO}_3)$:PTM] are very similar between 600 and 50 mab (Table 1), suggesting a similar source and chemical composition at both depths and supporting the possibility of a rebound phenomenon.

Another possible explanation for the increased particulate fluxes at 50 mab is overtrapping by the sediment traps at this depth where current flow is higher. Elevated current speeds will increase the collection rate of particles by conical sediment traps (Gust et al. 1992). Mean current speeds were 65% higher at 50 mab ($\bar{x} = 3.8 \text{ cm s}^{-1}$) than at 600 mab ($\bar{x} = 2.3 \text{ cm s}^{-1}$), but we have not observed any obvious seasonal variation in current flow between these two depths to explain the disparity in flux rates observed in summer between 600 and 50 mab. Gust et al. (1992) argued that the complexity of the hydrodynamics surrounding sediment traps precludes development of an algorithm to relate the flow field to trap collection efficiency, especially when

the flow velocity around the sediment traps exceeds the settling speed of particles.

Regardless of the mechanism(s) responsible for the observed increases in particulate fluxes at 50 mab during summer, further evaluation is necessary to explain the formation of large detrital aggregates and their subsequent appearance on the sea floor. We observed aggregations of particulate matter in the 600- and 50-mab sediment trap collections primarily in summer and fall, coinciding with periods when aggregates were observed on the sea floor in 1990 (Fig. 2) and suggesting that detrital aggregates have an origin outside the benthic boundary layer, possibly as a result of agglutination and sinking during phytoplankton blooms (Hill 1992). However, the difficulty in distinguishing aggregates produced naturally from those created or altered artificially after passing through the sediment trap baffle or during concentration in the collection cups must be considered (Gardner and Richardson 1992). The area of each opening in the sediment trap baffle (1 cm²) is less than that of most detrital aggregates we observed on the sea floor (0.6–191 cm²; \bar{x} = 18 cm²; Fig. 4). Asper (1987) photographed detrital aggregates ranging from 0.1 to 0.5 cm in diameter entering a sediment trap at 3,800 m in the Panama Basin. The detrital aggregates we observed on the sea floor were larger than those photographed in sediment traps by Asper (1987), suggesting that further agglutination may occur on or near the sea floor (Reimers and Wakefield 1989; Riemann 1989). However, we did not observe any movement or enlargement of detrital aggregates once on the sea floor, suggesting that further agglutination does not occur on the bottom.

Smaller particles might coalesce in the water column to form larger particles as a result of physical, chemical, and biological processes (e.g. McCave 1984), ultimately reaching the sizes of the aggregates we observed on the sea floor. Such interactions between fast-sinking aggregates produced in surface waters and suspended aggregates have been proposed as an explanation for the much higher mass fluxes and suspended mass concentrations estimated from photographic techniques with a profiling camera system compared to those estimated from sediment trap collections at abyssal depths in the Panama Basin (Asper et al. 1992).

The probability of a suspended particle attaching to a sinking particle increases with increasing particle volume, surface area of contact, and collision velocity (Alldredge and McGillivray 1991). Repackaging and aggregation of detrital aggregates also can be mediated by the ingestion and processing of detritus by zooplankton (Wishner and Gowing 1992), which increase in biomass near the sea floor (Wishner 1980; Childress et al. 1989; Smith 1992). This biologically mediated formation of detrital aggregates has been invoked to explain the downward flux of resuspended sediment as feces in the abyssal North Atlantic (Spencer et al. 1978). In the Panama Basin, there is a pronounced increase in the flux of fecal pellets in the bottom 1,000 m of the water column; this phenomenon has been attributed to deep lateral advection (Pilskaln and Honjo 1987). A combination of these physically and biologically mediated processes near the sea floor should produce a lag between the initial pulse of small particulate matter entering the benthic boundary layer and the arrival of larger detrital aggregates on the sea floor.

Sea floor—SCOC increased prior to the first observation of detrital aggregates on the sea floor in conjunction with spring pulses in particulate fluxes during 1990 (Fig. 2), suggesting that small sinking particles (POC) not visible in the time-lapse photographs may be the primary trophic link between the near-bottom pelagic and sediment communities at this station. Support for this interpretation comes from the size of the detrital aggregates and their distribution on the sea floor with respect to SCOC measurements.

SCOC, as a measure of the mineralization rate of organic matter by the sediment community, increased significantly [$P < 0.05$; $U_{0.01(2),6,7} = 39$, $U = 42$] between February and June 1990, immediately preceding the first observations of detrital aggregates on the sea floor in July (Fig. 2). A similar pattern appeared the following year, when the particulate flux peaked in April 1991, at least 1 month later than in 1990, corresponding to a sharp increase in SCOC between February and July 1991 and a peak in Chl *a* in the upper 2.5 mm of the sediment in June (Fig. 5). There was no evidence of detrital aggregates on the sea floor through the middle of July 1991, when our camera observations stopped. Given the lim-

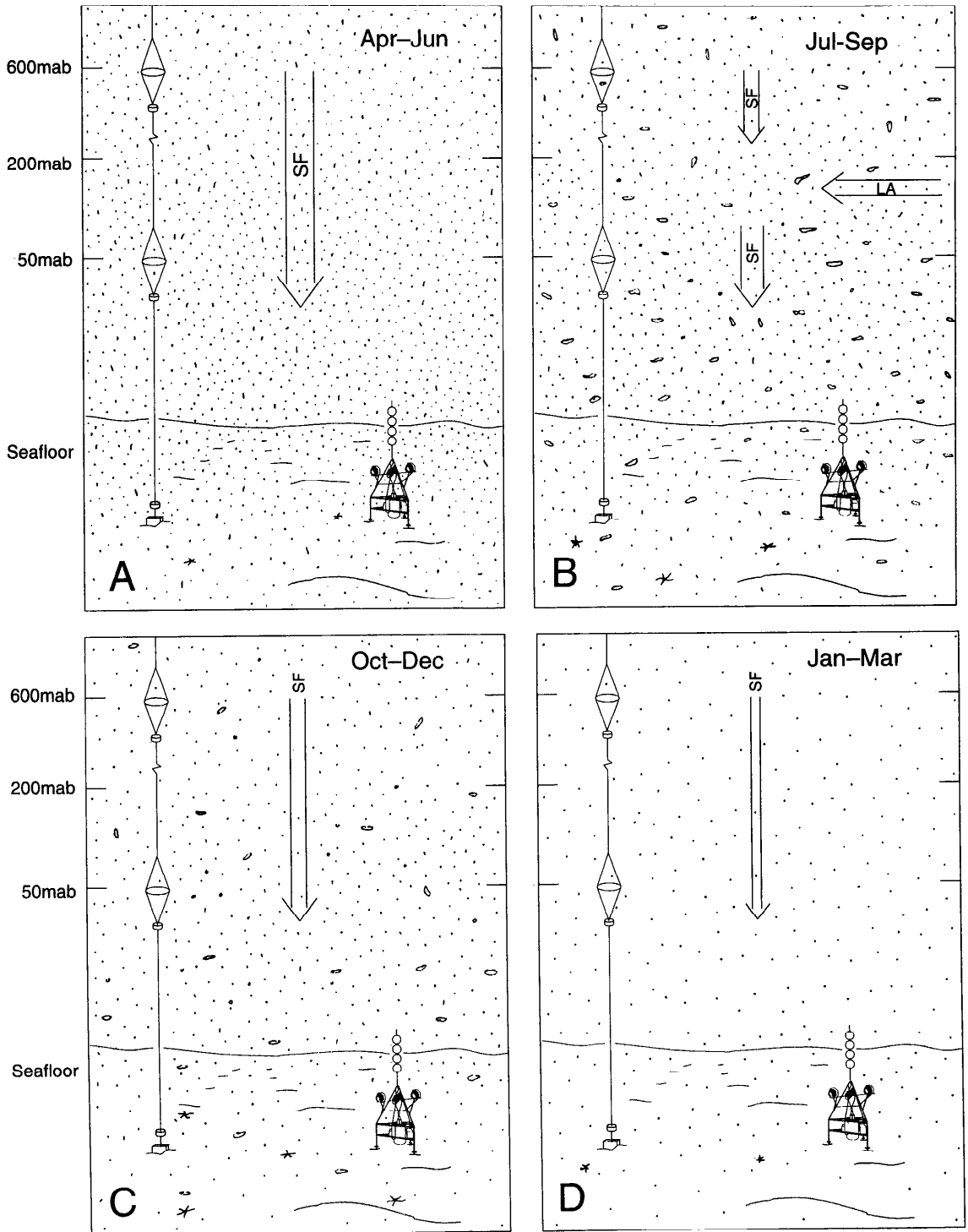


Fig. 7. Illustration of the scenario for coupling of near-bottom pelagic and benthic processes during four periods of the year. Sediment traps moored at 600 and 50 mab are illustrated along with the 200-mab horizon below which light transmission decreases. The camera tripod is shown on the sea floor. (SF—sinking flux; LA—lateral advection.)

ited area covered by the detrital aggregates on the sea floor (<1.5% at any one time; Fig. 2) and the probable restriction of their short-term effect on the sediment community to a localized area beneath and surrounding each aggregate, an immediate large-scale impact of these aggregates on the sediment biota, as reflected in SCOC or ATP concentrations, would not be expected.

Increased activity of the epibenthic megafauna coincided with observations of detrital aggregates on the sea floor, and megafauna were occasionally observed in association with detrital aggregates. Similar associations of megafauna with patches of detritus have been found in the North Atlantic (Lampitt 1985; Billett and Hansen 1982), and seasonality in the supply of detritus to the sea floor has been related to feeding in several deep-sea echinoderms (Thiel et al. 1989; Pearson and Gage 1984; Billett et al. 1988; Gooday and Turley 1990; Pfannkuche and Lochte 1993). Activity of sediment biota, including the epibenthic megafauna, is reflected in the high biological mixing coefficient ($D_B = 25.2 \text{ cm}^2 \text{ yr}^{-1}$) measured in the sediment at our abyssal station (Cai 1992).

Scenario for pelagic-benthic coupling—Given the measurements and observations reported above, we propose the following scenario for the coupling of near-bottom pelagic and benthic processes at this abyssal station (Sta. M). Spring pulses (April–June; Fig. 7A) of particulate matter enter the benthic boundary layer and settle directly to the sea floor as small particles undetectable by our camera system (<0.6 cm²). These small particles are “finely” dispersed, creating elevated concentrations of Chl *a* in the surface sediment and fueling an increase in the activity and biomass of sediment biota as estimated by measurements of SCOC and ATP taken with and from the randomly placed free-vehicle grab respirometer.

During summer (July–September; Fig. 7B), pulses of small particles combined with large aggregates (>0.6 cm²) enter the benthic boundary layer by sinking vertically from the overlying water column and by lateral advection. The sinking particulate matter is augmented by a persistent supply of small suspended particles and by laterally advected particles in the bottom 200 m of the water column. While in this concentrated suspen-

sion, coalescence of particles is enhanced, producing large detrital aggregates (>0.6 cm²) which, due to their increased density, settle out and appear as widely scattered patches on the sea floor. At the same time, smaller particles (<0.6 cm²) continue to fall to the sea floor, fueling the highest peaks in SCOC and sediment ATP concentrations during the year. The presence of the large detrital aggregates on the sea floor is synchronous with an increase in the activity of the mobile megafauna, primarily *A. abyssorum*. These active foragers disperse the particulate matter as feces or exuviae over large areas of the sea floor, temporally blending it into a spatial mosaic of sediment which supports a sediment community activity (and thus SCOC) largely indistinguishable from areas not impacted by detrital aggregates.

In fall (October–December; Fig. 7C), the lateral advection of particulate matter decreases, and fluxes of both small and large detrital aggregates to the sea floor decline. The dispersal and temporal and spatial blending of the large detrital aggregates by mobile megafaunal activity create elevated concentrations of organic C across the surface sediment, permitting sustained high rates of sediment community activity into fall, even when particulate fluxes are declining.

The winter period (January–March; Fig. 7D) is characterized by low fluxes of small particles; these particles settle to the sea floor and, in combination with organic C in the upper few centimeters of the sediment, sustain a lower level of SCOC. Large detrital aggregates are absent from the sea floor, and mobile megafaunal activity is depressed compared to other periods of the year.

Comparisons to other areas—Our results show a temporal relationship between the flux of particulate matter entering the benthic boundary layer and the arrival and residence on the sea floor of photographically detectable detritus in gradual increments over a 6-month period. This gradual supply of small detrital aggregates, sparsely distributed at any one time but collectively covering 24.8% of the sea floor annually, contrasts with the situation observed in the eastern North Atlantic at similar abyssal depths and temperate latitudes. The detrital aggregates in the North Atlantic form seasonal “carpets” that cover a large proportion of the sediment surface at any one time (Lampitt 1985) and are routinely sampled with surface

corers (Billett et al. 1983; Thiel et al. 1989; Rice et al. 1986). Bottom currents are of sufficient magnitude to move detrital aggregates and carpets across the sea floor and to resuspend this material at the North Atlantic sites (Lampitt 1985; Thiel et al. 1989), a physically much more dynamic environment than we have observed in the eastern North Pacific.

Detrital aggregates collected in the abyssal North Atlantic and incubated under simulated deep-sea conditions exhibited high microbial growth and decomposition rates (Lochte and Turley 1988; Gooday and Turley 1990), with an estimated decomposition rate of 1.8% of the available POC per day (Lochte and Turley 1988). Respiration of microorganisms colonizing detrital aggregates is estimated to contribute as much as 80% to the seasonal increase in SCOC measured in situ (Pfannkuche 1993). For a station at 1,430 m in the Norwegian Sea, SCOC measured on cores incubated under simulated deep-sea conditions showed a delayed response of ~30 d between a pulse in the POC flux (consisting of copepod fecal pellets) and an increase in SCOC (Graf 1989). However, the temporal resolution in these SCOC measurements was not sufficient to discount an earlier response in SCOC to the pulse in fecal pellets.

Our studies suggest a more efficient trophic coupling (i.e. higher utilization efficiency) between near-bottom pelagic and benthic processes in the eastern North Pacific where the seasonal supply of particulate matter occurs in small increments. This situation is different from that observed in the North Atlantic where detrital aggregates form seasonal carpets, a condition which, we speculate, should result in a lower utilization efficiency (defined as the ratio of the net production entering the benthic boundary layer to its assimilation by the benthic boundary layer community). Our continuing studies to characterize the particulate matter reaching the sea floor and to measure its utilization by the benthic boundary layer community will permit us to more critically evaluate the efficiency of trophic coupling in the deep ocean.

References

- ALLDREDGE, A. L., AND P. MCGILLIVARY. 1991. The attachment probabilities of marine snow and their

- implications for particle coagulation in the ocean. *Deep-Sea Res.* **38**: 431–443.
- ASPER, V. L. 1987. Measuring the flux and sinking speed of marine snow aggregates. *Deep-Sea Res.* **34**: 1–17.
- , S. HONJO, AND T. H. ORSI. 1992. Distribution and transport of marine snow aggregates in the Panama Basin. *Deep-Sea Res.* **39**: 939–952.
- BARTZ, J. R., R. V. ZANEVELD, AND H. PAK. 1978. A transmissometer for profiling and moored observations in water, p. 102–108. *In* *Ocean Optics 5*, Proc. SPIE 160.
- BILLETT, D. S. M., AND B. HANSEN. 1982. Abyssal aggregations of *Kolga hyalina* Danielsen and Koren (Echinodermata: Holothuroidea) in the northeast Atlantic Ocean: A preliminary report. *Deep-Sea Res.* **29**: 799–818.
- , R. S. LAMPITT, A. L. RICE, AND R. F. C. MANTOURA. 1983. Seasonal sedimentation of phytoplankton in the deep-sea benthos. *Nature* **302**: 520–522.
- , C. LLEWELLYN, AND J. WATSON. 1988. Are deep-sea holothurians selective feeders?, p. 421–429. *In* R. D. Burke et al. [eds.], *Echinoderm biology*. Balkema.
- BRODY, S. 1945. Bioenergetics and growth. Hafner.
- BRULAND, K. W., R. P. FRANKS, W. M. LANDING, AND A. SOUTAR. 1981. Southern California inner basin sediment trap calibration. *Earth Planet. Sci. Lett.* **53**: 400–408.
- BUCKLAND, S. T., D. R. ANDERSON, K. P. BURNHAM, AND J. L. LAAKE. 1993. Distance sampling: Estimating abundance of biological populations. Chapman and Hall.
- CAI, W.-J. 1992. In situ microelectrode studies of the early diagenesis of organic carbon and CaCO₃ in hemipelagic sediments of the northeast Pacific Ocean. Ph.D. thesis, Univ. California, San Diego. 238 p.
- CHILDRESS, J. J., D. L. GLUCK, R. S. CARNEY, AND M. M. GOWING. 1989. Benthopelagic biomass distribution and oxygen consumption in a deep-sea benthic boundary layer dominated by gelatinous organisms. *Limnol. Oceanogr.* **34**: 913–930.
- CRAVEN, D. B., R. A. JAHNKE, AND A. F. CARLUCCI. 1986. Fine-scale vertical distributions of microbial biomass and activity in California Borderland sediments. *Deep-Sea Res.* **33**: 379–390.
- , AND D. M. KARL. 1984. Microbial RNA and DNA synthesis in marine sediments. *Mar. Biol.* **83**: 129–139.
- CUSHING, D. H. 1982. *Climate and fisheries*. Academic.
- DEUSER, W. G. 1986. Seasonal and interannual variations in deep-water particle fluxes in the Sargasso Sea and their relation to surface hydrography. *Deep-Sea Res.* **33**: 225–246.
- , E. H. ROSS, AND R. F. ANDERSON. 1981. Seasonality in the supply of sediment to the deep Sargasso Sea and the implications for the rapid transfer of matter to the deep ocean. *Deep-Sea Res.* **28**: 495–505.
- DYMOND, J., AND OTHERS. 1981. A sediment trap inter-comparison study in the Santa Barbara Basin. *Earth Planet. Sci. Lett.* **53**: 409–418.
- FISCHER, K. M. 1984. Particle fluxes in the eastern tropical Pacific Ocean—sources and processes. Ph.D. thesis, Oregon State Univ. 225 p.
- GAGE, J. D. 1991. Biological rates in the deep sea: A

- perspective from studies on processes in the benthic boundary layer. *Rev. Aquat. Sci.* **5**: 49–100.
- GARDNER, W. D., AND M. J. RICHARDSON. 1992. Particle export and resuspension fluxes in the western North Atlantic, p. 339–364. *In* G. T. Rowe and V. Pariente [eds.], *Deep-sea food chains and the global carbon cycle*. Kluwer.
- , L. G. SULLIVAN, AND E. M. THORNDIKE. 1984. Long-term photographic, current, and nephelometer observations of manganese nodule environments in the Pacific. *Earth Planet. Sci. Lett.* **70**: 95–109.
- , AND I. D. WALSH. 1990. Distribution of macro-aggregates and fine-grained particles across a continental margin and their potential role in fluxes. *Deep-Sea Res.* **37**: 401–411.
- GOODAY, A. J., AND C. M. TURLEY. 1990. Responses by benthic organisms to inputs of organic material to the ocean floor: A review. *Phil. Trans. R. Soc. Lond. Ser. A* **331**: 119–138.
- GRAF, G. 1989. Benthic-pelagic coupling in a deep-sea benthic community. *Nature* **341**: 437–439.
- GUST, G., R. H. BYRNE, R. E. BERNSTEIN, P. R. BETZER, AND W. BOWLES. 1992. Particle fluxes and moving fluids: Experience from synchronous trap collections in the Sargasso Sea. *Deep-Sea Res.* **39**: 1071–1083.
- HEIP, C., B. F. KEEGAN, AND J. R. LEWIS. 1987. Long-term changes in coastal benthic communities. *Junk*.
- HILL, P. S. 1992. Reconciling aggregation theory with observed vertical fluxes following phytoplankton blooms. *J. Geophys. Res.* **97**: 2295–2308.
- HONJO, S. 1982. Seasonality and interaction of biogenic and lithogenic particulate flux at the Panama Basin. *Science* **218**: 883–884.
- , AND K. W. DOHERTY. 1988. Large aperture time-series sediment traps; design objectives, construction and application. *Deep-Sea Res.* **35**: 133–149.
- , AND S. J. MANGANINI. 1993. Annual biogenic particle fluxes to the interior of the North Atlantic Ocean; studied at 34°N 21°W and 48°N 21°W. *Deep-Sea Res.* **2** **40**: 587–607.
- , D. W. SPENCER, AND J. W. FARRINGTON. 1982. Deep advective transport of lithogenic particles in Panama Basin. *Science* **216**: 516–518.
- , ———, AND W. D. GARDNER. 1992. A sediment trap intercomparison experiment in the Panama Basin, 1979. *Deep-Sea Res.* **39**: 333–358.
- KARL, D. M., AND D. B. CRAVEN. 1980. Effects of alkaline phosphatase activity on nucleotide measurements in aquatic microbial communities. *Appl. Environ. Microbiol.* **40**: 549–561.
- KAUFMANN, R. S., W. W. WAKEFIELD, AND A. GENIN. 1989. Distribution of epibenthic megafauna and lebensspuren on two central North Pacific seamounts. *Deep-Sea Res.* **36**: 1863–1896.
- LAAKE, J. L., S. T. BUCKLAND, D. R. ANDERSON, AND K. P. BURNHAM. 1991. Distance sampling: Abundance estimation of biological populations. *DISTANCE user's guide*, 53 p.
- LAMPITT, R. S. 1985. Evidence for the seasonal deposition of detritus to the deep-sea floor and its subsequent resuspension. *Deep-Sea Res.* **32**: 885–897.
- LIKENS, G. E. 1989. Long-term studies in ecology: Approaches and alternatives. Springer.
- LOCHTE, K., AND C. M. TURLEY. 1988. Bacteria and cyanobacteria associated with phytodetritus in the deep sea. *Nature* **333**: 67–69.
- LONSDALE, P., AND J. B. SOUTHARD. 1974. Experimental erosion of North Pacific red clay. *Mar. Geol.* **17**: M51–M60.
- MCCAVE, I. N. 1984. Size spectra and aggregation of suspended particles in the deep ocean. *Deep-Sea Res.* **31**: 329–352.
- MICHAELSEN, J., X. ZHANG, AND R. C. SMITH. 1988. Variability of pigment biomass in the California Current System as determined by satellite imagery. 2. Temporal variability. *J. Geophys. Res.* **93**: 10,883–10,896.
- PARSONS, T. R., Y. MAITA, AND C. M. LALLI. 1984. A manual of chemical and biological methods for seawater analysis. Pergamon.
- PEARSON, M., AND J. D. GAGE. 1984. Diets of some deep-sea brittle stars in the Rockall Trough. *Mar. Biol.* **82**: 247–258.
- PELAEZ, J., AND J. A. MCGOWAN. 1986. Phytoplankton pigment patterns in the California Current as determined by satellite. *Limnol. Oceanogr.* **31**: 927–950.
- PFANNKUCHE, O. 1993. Benthic response to the sedimentation of particulate organic matter at the BIOTRANS station, 47°N, 20°W. *Deep-Sea Res.* **2** **40**: 135–149.
- , AND K. LOCHTE. 1993. Open ocean pelago-benthic coupling: Cyanobacteria as tracers of sedimenting salp faeces. *Deep-Sea Res.* **1** **40**: 727–737.
- PILSKALN, C. H., AND S. HONJO. 1987. The fecal pellet fraction of biogeochemical particle fluxes to the deep sea. *Global Biogeochem. Cycles.* **1**: 31–48.
- REIMERS, C. E., R. A. JAHNKE, AND D. C. MCCORKLE. 1992. Carbon fluxes and burial rates over the continental slope and rise off central California with implications for the global carbon cycle. *Global Biogeochem. Cycles* **6**: 199–224.
- , AND K. L. SMITH, JR. 1986. Reconciling measured and predicted fluxes of oxygen across the deep sea sediment-water interface. *Limnol. Oceanogr.* **31**: 305–318.
- , AND W. W. WAKEFIELD. 1989. Flocculation of siliceous detritus on the sea floor of a deep Pacific seamount. *Deep-Sea Res.* **36**: 1841–1861.
- RICE, A. L., AND OTHERS. 1986. Seasonal deposition of phytodetritus to the deep-sea floor. *Proc. R. Soc. Edinburgh* **88B**: 265–279.
- RIEMANN, F. 1989. Gelatinous phytoplankton detritus aggregates on the Atlantic deep-sea bed: Structure and mode of formation. *Mar. Biol.* **100**: 533–539.
- SMITH, K. L., JR. 1987. Food energy supply and demand: A discrepancy between particulate organic carbon flux and sediment community oxygen consumption in the deep ocean. *Limnol. Oceanogr.* **32**: 201–220.
- . 1992. Benthic boundary layer communities and carbon cycling at abyssal depths in the central North Pacific. *Limnol. Oceanogr.* **37**: 1034–1056.
- , R. J. BALDWIN, AND P. M. WILLIAMS. 1992. Reconciling particulate organic carbon flux and sediment community oxygen consumption in the deep North Pacific. *Nature* **359**: 313–316.
- , R. S. KAUFMANN, AND W. W. WAKEFIELD. 1993. Mobile megafaunal activity monitored with a time-

- lapse camera in the abyssal North Pacific. *Deep-Sea Res.* 1 **40**: 2307–2324.
- SMITH, R. C., X. ZHANG, AND J. MICHAELSEN. 1988. Variability of pigment biomass in the California Current System as determined by satellite imagery. 1. Spatial variability. *J. Geophys. Res.* **93**: 10,863–10,882.
- SPENCER, D. W., AND OTHERS. 1978. Chemical fluxes from a sediment trap experiment in the deep Sargasso Sea. *J. Mar. Res.* **36**: 493–523.
- STRICKLAND, J. D. H., AND T. R. PARSONS. 1972. A practical handbook of seawater analysis, 2nd ed. *Bull. Fish. Res. Bd. Can.* 167.
- THIEL, H., AND OTHERS. 1989. Phytodetritus on the deep-sea floor in a central oceanic region of the northeast Atlantic. *Biol. Oceanogr.* **6**: 203–239.
- TOWNSEND, D. W., AND L. M. CAMMEN. 1988. Potential importance of the timing of spring plankton blooms to benthic-pelagic coupling and recruitment of juvenile demersal fishes. *Biol. Oceanogr.* **5**: 215–229.
- TYLER, P. A. 1988. Seasonality in the deep sea. *Oceanogr. Mar. Biol. Annu. Rev.* **26**: 227–258.
- WAKEFIELD, W. W., AND A. GENIN. 1987. The use of a Canadian (perspective) grid in deep-sea photography. *Deep-Sea Res.* **34**: 469–478.
- WALSH, I., K. FISCHER, D. MURRAY, AND J. DYMOND. 1988. Evidence for resuspension of rebound particles from near-bottom sediment traps. *Deep-Sea Res.* **35**: 59–70.
- , AND W. D. GARDNER. 1992. A comparison of aggregate profiles with sediment trap fluxes. *Deep-Sea Res.* **39**: 1817–1834.
- WISHNER, K. F. 1980. The biomass of the deep-sea benthopelagic plankton. *Deep-Sea Res.* **27**: 203–216.
- , AND M. M. GOWING. 1992. The role of deep-sea zooplankton in carbon cycles, p. 29–43. *In* G. T. Rowe and V. Pariente [eds.], *Deep-sea food chains and the global carbon cycle*. Kluwer.
- WOLF, P. R. 1983. *Elements of photogrammetry: With air photo interpretation and remote sensing*. McGraw-Hill.
- ZAR, J. H. 1984. *Biostatistical analysis*. Prentice-Hall.

Submitted: 18 February 1993

Accepted: 12 July 1993

Amended: 13 September 1993